IMM 374
NYO-1480-111
February 1969

Courant Institute of
Mathematical Sciences

Stresses in Cantilever Plates

Frances Bauer and Edward L. Reiss

Prepared under Contract AT(30-1)-1480
with the U.S. Atomic Energy Commission
and Contract Nonr-285(42) with the
Office of Naval Research NR 064-438

Distribution of this document is unlimited.

IMM 374
C.1

New York University

NEW YORK UNIVERSITY
COURANT INSTITUTE - LIBRARY
251 Mercer St. New York, N.Y. 10012

NR 064-438

IMM 374
NYO-1480-111
February 1969

New York University

Courant Institute of Mathematical Sciences

STRESSES IN CANTILEVER PLATES

Frances Bauer and Edward L. Reiss

This report represents results obtained at the Courant Institute of Mathematical Sciences, New York University, with the U.S. Atomic Energy Commission, Contract AT(30-1)-1480 and the Office of Naval Research, Contract Nonr-285(42).
Reproduction in whole or in part is permitted for any purpose of the United States Government.

Distribution of this document is unlimited.

NEW YORK UNIVERSITY
COURANT INSTITUTE-LIBRARY

Abstract

Key Words: Cantilever Plates, Numerical Methods, Plates.

A numerical method is presented for determining the bending stresses in elastic cantilever plates. Southwell's formulation of the classical small deflection plate theory is employed. The method is applied to obtain numerical solutions for rectangular and swept back plates subjected to a variety of surface and edge loads. Boundary layer effects are observed for the uniformly loaded rectangular plates as the length of the plate decreases. The effects of a load concentration and sweep back are observed and summarized in the form of stress concentration factors.

1. Introduction.

The determination of the stresses in elastic cantilever plates is required for a variety of structural applications. The plate is clamped on a segment C of the boundary curve B. On $B' \equiv B - C$, the normal bending moment M_n and the shear reaction V_n are specified. The face of the plate is subjected to a normal pressure $p(x,y)$.

The applied forces M_n, V_n and p and the thickness of the plate are sufficiently small so that the classical small deflection, Lagrange-Kirchhoff theory of plates [1] is valid. In its conventional formulation, this theory requires the solution of a biharmonic boundary value problem for the normal displacement $w(x,y)$ of the midplane of the plate. The boundary conditions are that w and its first normal derivative vanish on C, and two linear combinations of the second and third derivatives of w are specified on B'.

Southwell's [2] formulation of the classical theory yields a boundary value problem for a system of three second order partial differential equations for three dependent variables $\phi(x,y)$, $u(x,y)$ and $v(x,y)$. The function ϕ is a solution of a boundary value problem for Poisson's equation and is determined independently of u and v. The remaining two equations for u and v are coupled. They are similar to the displacement equations of equilibrium for either plane stress or plane strain [4]. The function ϕ appears in the inhomogeneous terms in these equations. The boundary conditions on B' are that u and v are specified, i.e. Dirichlet conditions are specified on B'. Thus in Southwell's

formulation the complicated higher order derivative boundary conditions on B' of the classical formulation are replaced by simple conditions. This is especially important for the analysis in this paper since finite difference methods are easily and accurately applied to Dirichlet conditions. A discussion of difference and other approximate methods for cantilever plates and references to previous work are given in [1] and [3]. Southwell's formulation has been extended [5] to plates of variable thickness. Numerical solutions are obtained in [5] by employing relaxation methods.

In this paper an accelerated iteration method is presented for solving cantilever problems using Southwell's formulation. The method was previously used in studies of the nonlinear deformations of elastic plates [6,7,8] and other problems. Each iterate, is determined as the solution of a boundary value problem for Poisson's equation. The iterates are numerically evaluated by approximating this boundary value problem by difference equations. The resulting system of linear algebraic equations which is of quasi-tridiagonal form is solved by a direct factoring method [9]. The method can also be considered as an iterative procedure for solving the difference equations which are obtained from the original plate boundary value problem. In previous applications of difference methods*, coarse meshes, e.g. $\delta = L/2$ were employed. Here δ is the mesh width and L is a

* See e.g. [1,3].

minimum diameter of the plate. The present computations indicate that mesh widths as small as $\delta = L/52$ may be required to accurately estimate the stresses. The finer meshes are more important for irregular domains such as the swept back plate considered in this paper; see Figure 1.

In Section 5 the iterative method is applied to obtain numerical solutions for rectangular plates and the swept back plate shown in Figure 1 subjected to a variety of loads. It is shown that the solution of the infinite strip cantilever provides a reasonably good estimate of the numerically determined maximum moment for the symmetrically loaded rectangular plates that are analyzed in Section 5. It is an underestimate and improves as the plate is made narrower. The infinite strip cantilever gives an inaccurate approximation for unsymmetric loading. For equivalent loading conditions, the maximum moment on the clamped edge is larger for the swept back plate than for the rectangular plate with the same aspect ratio. Various stress concentration factors that indicate the relative effects of sweep back and unsymmetrical loading are presented.

2. Formulation.

The midplane of the plate covers the region R in the right half of the x,y plane. The boundary B of R is a positively oriented, simple, closed contour with arc length s. The unit outward normal to B is $\underset{\sim}{n} = (a,b)$ and the unit tangent vector is

$\underset{\sim}{t} = (-b,a)$. Here a and b are the direction cosines of $\underset{\sim}{n}$. The boundary contains the straight line C: $x = 0$, $y_0 \leq y \leq y_1$. The plate is clamped on C. On $B' \equiv B - C$, the normal bending moment $M_n = M(s)$ and the transverse shear reaction $V_n = V(s)$ where M and V are prescribed functions. An arc of B' is free if $M = V \equiv 0$ on that arc. A pressure $p(x,y)$ is applied normal to the x,y plane. The applied loads p, M, V and the region R are referred to as the data.

The x and y bending moments are denoted by M_x and M_y and the twisting moment by $M_{xy} = -M_{yx}$. They are related to the normal displacement $w(x,y)$ of the midplane by*

$$M_x = -D(w_{xx} + w_{yy}), \quad M_y = -D(w_{yy} + \nu\, w_{xx}), \quad M_{xy} = D(1-\nu)w_{xy}, \qquad (1a,b,c)$$

where ν is Poisson's ratio and D is the flexural rigidity of the plate. On B', M_n and V_n are related to M_x, M_y and M_{xy} by [1],

$$M_n \equiv 2\, M_{xy}ab - M_x a^2 - M_y b^2 , \quad V_n \equiv Q_n - \frac{\partial}{\partial s} M_{ns} , \qquad (2)$$

where

$$M_{ns} \equiv (M_x - M_y)ab + M_{xy}(a^2 - b^2) ,$$

$$Q_n \equiv (\frac{\partial}{\partial x} M_x - \frac{\partial}{\partial y} M_{xy})a + (\frac{\partial}{\partial y} M_y - \frac{\partial}{\partial x} M_{xy})b , \qquad (3)$$

---

* Here and in the remainder of the paper the following notation is used: subscripts on capital letters such as M, Q and V are indices; subscripts on lower case letters such as u, v, w and ϕ denote partial derivatives.

and the notation $\partial f/\partial s \equiv \underset{\sim}{t} \cdot \nabla f$ is used for the tangential derivative of f.

Let $\phi(x,y)$ be the unique solution of

$$\Delta\phi = -p \ , \quad \text{for} \quad x,y \text{ in } R \ ;$$
$$\phi = 0, \text{ on } C; \quad \phi_n \equiv \underset{\sim}{n} \cdot \nabla\phi = -V, \text{ on } B' \ . \tag{4}$$

Here Δ is the two dimensional Laplacian. The boundary value problem (4) is called Problem ϕ. The moment potentials $u(x,y)$ and $v(x,y)$ are defined by

$$M_x = v_y - \phi \ , \quad M_y = u_x - \phi \ , \quad M_{xy} = (v_x + u_y)/2 \ . \tag{5}$$

The differential equations of Southwell's formulation [2] are then given by,

$$\Delta \underset{\sim}{u} = k\nabla(-\nabla \cdot \underset{\sim}{u} + 2\phi) \ , \quad k \equiv (1-\nu)/(1+\nu) \ , \tag{6}$$

where $\underset{\sim}{u}$ is the vector with components u and v and ∇ is the two dimensional gradient operator. They are analogous to the displacement equilibrium equations of plane stress and plane strain, where $\underset{\sim}{u}$ is then the displacement vector, $\nabla\phi$ is proportional to the body force and k is a different function of ν.

The boundary conditions are,

$$w = w_x = 0 \ , \quad \text{on } C \ , \tag{7}$$

$$M_n = M(s) \ , \quad V_n = V(s) \ , \quad \text{on } B' \ . \tag{8}$$

They are expressed in terms of $\underset{\sim}{u}$ and ϕ by first observing that (7) implies that $w_{yy} = w_{xy} = 0$ on C. Substituting this result and (3) in (1) gives the required boundary conditions on C as

$$u_x - \nu v_y = u_y + v_x = 0 \ . \tag{9}$$

Conversely, if $\underset{\sim}{u}$ satisfies (9) then from (5) and (1) it follows that C is clamped within a rigid rotation. When (5), (2) and (3) are inserted in (8), then (8) is reduced to

$$\underset{\sim}{t} \cdot \underset{\sim}{u}_s = \phi - M \ , \quad \frac{\partial}{\partial s} (\underset{\sim}{n} \cdot \underset{\sim}{u}_s) = 0 \ . \tag{10a,b}$$

Here the notation $\underset{\sim}{u}_s$ is used for the vector with components u_s and v_s. Equation (10b) is integrated with respect to s and the resulting equation and (10a) are solved for $\underset{\sim}{u}_s$. Integrating $\underset{\sim}{u}_s$ gives

$$\underset{\sim}{u} = \int_0^s (\phi - M)\underset{\sim}{t} \, ds \ , \quad \text{on } B' \ . \tag{11}$$

The three constants of integration are set equal to zero since they correspond to solutions which have vanishing bending moments.

Problem P is defined as the boundary value problem which consists of determining a vector $\underset{\sim}{u}$ that satisfies (6), (9) and (11). The solution of Problem ϕ is used to determine the inhomogeneous terms in Problem P. When solutions of Problems ϕ and P are obtained the moments are determined from (5). The normal displacement can then be evaluated by solving (1) for the

second derivatives of w and then integrating these expressions using (7). Since we are primarily interested in the moments, these integrals are not evaluated. An important advantage of Southwell's formulation is that the complicated higher order derivative conditions on B' of the classical formulation are replaced by the simple Dirichlet conditions (11).

At the corners x = 0, and y = y_0, y_1, the boundary conditions are not uniquely prescribed; see (9) and (11). Thus we expect a singularity in the solution of Problem P or its derivatives at the corners. The moments may be discontinuous and even unbounded at these points. The numerical results discussed in Section 5 indicate that this might occur for the specific problems investigated.

3. The Iterative Method.

An approximate solution of Problem P is obtained by the following iterative method. Starting from an initial estimate $\underset{\sim}{u}^0(x,y)$ of the solution for fixed data, a sequence of iterates $\underset{\sim}{u}^1(x,y)$, $\underset{\sim}{u}^2(x,y)$,..., is defined by the recursions

$$\Delta\bar{\underset{\sim}{u}}^n = k\nabla(-\nabla\cdot\underset{\sim}{u}^{n-1} + 2\phi) \ , \quad x,y \text{ in } R \ , \tag{1a}$$

$$\bar{u}_x^n = \nu\, v_y^{n-1} \ , \quad \bar{v}_x^n = -u_y^{n-1} \ , \quad \text{on } C \ , \tag{1b}$$

$$\bar{\underset{\sim}{u}}^n = \int_0^s (\phi - M)\underset{\sim}{t}\, ds \ , \quad \text{on } B' \ , \tag{1c}$$

$$\underset{\sim}{u}^n = \theta\, \bar{\underset{\sim}{u}}^n + (1-\theta)\underset{\sim}{u}^{n-1} \ , \quad \text{in } R+B \ . \tag{1d}$$

Here θ is the acceleration parameter. The vector $\underset{\sim}{\overline{u}}^n$ is a provisional iterate. The function ϕ in (1) is a solution of Problem $\frac{1}{2}$. We assume, for the present, that it is known.

Each iterate in (1) is determined by solving the boundary value problem

$$\begin{aligned} \Delta q &= f(x,y) \ , \quad \text{for } x,y \text{ in } R \ , \\ q_x &= h(y) \ , \quad \text{on } C \ , \quad q = g(s) \quad \text{for } x,y \text{ on } B' \ . \end{aligned} \tag{2}$$

Here f, g and h are determined by ϕ, the data and previous iterates. An approximate solution of (2) is obtained by a difference method similar to the one employed in [7,8,10]. The region R is covered with a rectilinear mesh with uniform mesh spacing δ in the x and y directions. In this paper two regions R are considered. One of them is the rectangle and the other is the swept back plate shown in Figure 1. When R is a rectangle then the mesh is selected so that mesh lines coincide with the edges of the rectangle. When R is the region shown in Figure 1, then $x = 0, 1$ and $y = 0, 1$ are taken as mesh lines and each mesh line with $1 > y > a$ has a point on the skew edge. For more complicated regions it may not always be possible to select a uniform mesh such that mesh points coincide with the boundary. Special approximations are then required at the boundary.

There are $I+1$ and $J+1$ lines in the x and y directions so that

$$I = \ell_x/\delta \ , \quad J = \ell_y/\delta \ . \tag{3}$$

When R is a rectangle, ℓ_x and ℓ_y are the lengths of the sides. When R is the region shown in Figure 1 then $\ell_x = \ell_y = 1$. The mesh points (x_i, y_j) are defined by

$$\begin{aligned} x_i &= i\,\delta\,, \quad i = 0,\ldots,I\,, \\ y_j &= j\,\delta\,, \quad j = 0,\ldots,J\,. \end{aligned} \tag{4}$$

The set of mesh points which are in R is called R_δ. Likewise, the set of mesh points on B' is called B'_δ and the set of mesh points on C is called C_δ. The end points $x = 0$, $y = y_0$ and $x = 0$, $y = y_1$ are assumed to be in C_δ. A function defined only at the points of the mesh is called a mesh function. It is assumed that at each point x_i, y_j of $R_\delta + B'_\delta + C_\delta$ the solution of (2), $q(x_i, y_j)$, is approximated by the mesh function q_{ij} which solves the difference equations

$$\Delta_\delta q_{ij} = f_{ij}\,, \qquad (x_i, y_j) \in R_\delta\,, \tag{5a}$$

$$q_{ij} = g_{ij}\,, \qquad (x_i, y_j) \in B'_\delta\,, \tag{5b}$$

$$D_\delta q_{ij} = h_{ij}\,, \qquad (0, y_j) \in C_\delta\,. \tag{5c}$$

In (5) the following notation is used. The mesh function $\{g_{ij}\}$ is defined only for points x_i, y_j in B'_δ. It is evaluated by approximating the integrals on the right side of (1c) by Simpson's rule. The mesh function $\{h_{ij}\}$ is defined only for points 0, y_j in C_δ. It is evaluated by approximating the derivatives on the

right side of (1b) by a centered difference formula. When R is a rectangle the mesh function $\{f_{ij}\}$ is obtained by approximating the derivatives in the right hand side of (1a) by centered difference formulae. If R is the region in Figure 1, then centered difference formulae are used everywhere except in approximating the mixed second derivative along the diagonal line S_δ which consists of the mesh points one point to the left of the skew edge. There a special inward difference formula, with the same truncation error as the centered approximation, is used to avoid introducing mesh points exterior to R. Several different inward formulae were employed. They gave only insignificant changes in the numerical results. The difference operator D_δ in (5c) is the forward three point difference approximation of $O(\delta^2)$ of $\partial/\partial x$. In (5a) Δ_δ is the nine point difference approximation of the Laplacian for $x_i, y_j \in R_\delta - S_\delta$. On S_δ the usual five point Laplace difference operator is used. This again avoids the introduction of mesh points exterior to R that are required if the nine point formula is employed on S_δ. The solution of the difference equations is presumably an accurate approximation of the solution of (2) for sufficiently small δ.

The difference equations (5) are a system of linear algebraic equations for the mesh function $\{q_{ij}\}$. The coefficient matrix is tridiagonal with respect to matrices. The system is solved by a direct factorization method [9]. Some of the details of the application of the factorization method are discussed in [7].

Problem ϕ, (2.4), is solved numerically in the same way as (2). The resulting algebraic equations are also tridiagonal with respect to matrices. They are solved by the factorization method [9]. The numerical solution of Problem ϕ is used to compute the inhomogeneous terms in (1).

When the iterations (1) have converged, the moments are computed from difference approximations of (2.5).

4. Computing Methods.*

A sufficiently small value of the mesh spacing δ was determined by performing a sequence of test calculations with successively finer meshes. Mesh sizes of $\delta = 1/10$, $1/13$, $1/26$, $1/40$ and $\delta = 1/52$ were used. For the rectangle the mesh size $\delta = 1/13$ was satisfactory. The test calculations for the swept back plate indicate that the $\delta = 1/52$ mesh and perhaps a finer mesh is required. The agreement between the results for $\delta = 1/26$ and $\delta = 1/52$ is good for mesh points away from the corners $x = y = 0$ and $x = 0$, $y = 1$. Within 3 or 4 mesh points of the corners the results are significantly different.**

---

* The computations were performed on the CDC 6600 computer at the AEC Computing and Applied Mathematics Center of the Courant Institute of Mathematical Sciences. In all the calculations $\nu = 0.32$ was used.

** Cf. the comments in Section 5.

The following numerical convergence criterion was employed:

$$\max_{(x_i,y_j)\in R_\delta+B_\delta} \{|u_{ij}^n - u_{ij}^{n-1}|, |v_{ij}^n - v_{ij}^{n-1}|\} < 10^{-\delta} . \qquad (1)$$

In a test calculation the right hand side of (1) was decreased. This introduced only insignificant changes in the answers. The condition (1) is only necessary for convergence.

Starting from a fixed initial iterate, the number of iterations needed to satisfy (1) depends on the value of the acceleration parameter θ in (3.1). The optimal value, θ_0, to use is the one that minimizes the number of iterations for convergence. Estimates for θ_0 were obtained from a series of test calculations. For the problems considered $\theta = 0.6$ was a satisfactory value.

The number of iterations for convergence varies with the data of the problem and the choice of θ and δ. For most problems approximately 400 iterations were required. For a mesh with 676 points the iterations take approximately one minute of CDC 6600 time.

5. Applications of the Method and Summary of the Results.

Some of the numerical results will be compared with the exact solution of the infinite strip cantilever $0 \leq x \leq \ell$, $|y| < \infty$, with the loads independent of y. Its solution which is indicated by a superscript i is given by,

$$M_x^i = \int_x^{\ell} (\xi - x)p(\xi)\, d\xi - (\ell - x)V \ , \quad M_y^i = \nu\, M_x^i \ , \quad M_{xy}^i = 0 \ . \qquad (1)$$

We assume that $M \equiv 0$ in (3.1c) for all the problems studied.

The rectangular plates are of length ℓ in the x direction and $y_0 = -y_1 = -1$. If p and V are symmetric in y with respect to $y = 0$, then M_x and M_y are symmetric and M_{xy} is antisymmetric. The square cantilever, $\ell = 2$, with $p \equiv 1$ and $V \equiv 0$ is considered first. Thus B' is free. The results shown in Figures 2 and 3 are obtained with $\delta = 1/13$. The maximum moment obtained with this mesh is $M_x(0,\pm 2/13) \approx -2.135$. The graphs in Figures 2 indicate that M_x^i is an accurate approximation for $x \geq 0.3$. Near $x = 0$ it approximates $M_x(x,0)$ more accurately than it approximates $M_x(x,-12/13)$. M_{xy} is usually much smaller that the other moments and $M_{xy}^i \equiv 0$. The bending moments on the clamped edge C are graphed in Figure 3. The approximation (1) is accurate in the interior of C. For example, it underestimates $M_x(0,0)$ by less than 6.5 percent.

Graphs of M_x on the clamped edge for uniformly loaded, $p \equiv 1$, $V \equiv 0$, rectangular plates with $\ell = 1,2$(square) 4 are shown in Figure 4. The numerical values of $M_x(0,0)$ and $M_x^i(0)$ are summarized in Table I.

Table I. Rectangular Plates, $p \equiv 1$, $V \equiv 0$.

ℓ	δ	$-M_x(0,0)$	$-M_x^1(0)$	% error
1	1/20	.514	0.5	-2.92
2	1/10	2.135	2.0	-6.32
2	1/13	2.135	2.0	-6.32
2	1/20	2.136	2.0	-6.37
4	1/10	8.968	8.0	-10.8

For the wide plate $\ell = 1$, $M_x(0,y)$ and also $M_y(0,y)$ (not shown) have three stationary points. For the long plate $\ell = 4$ and the square plate $\ell = 2$, the same quantities have a single minimum. The approximation (1) is more accurate at $x = 0$ for a larger range of y values for $\ell = 1$ than for $\ell = 2$ and $\ell = 4$. In fact, we conjecture that as $\ell \to 0$ the solution of Problem P with $p \equiv 1$ and $V = 0$ approaches (1) in the interior of the rectangle. Near $y = \pm 1$ there is a boundary layer in which the solution varies rapidly from (1) so as to satisfy the boundary conditions on $y = \pm 1$.

The values of $M_x(0,y)$ for $\ell = 2$ and $\delta = 1/10$ and $\delta = 1/20$ are in good agreement for y away from the edges $y = \pm 1$. The values of $M_x(0,\pm 1)$ for a sequence of mesh widths are listed in Table II.

Table II. Corner Moments for the Square Plate, $p \equiv 1$, $V \equiv 0$.

δ	1/10	1/13	1/20
$M_x(0,\pm 1)$	-.460	-.269	+.037

The values of $M_x(0,\pm 1)$ increase as δ decreases. Because of the singularity at $x = 0$, $y = \pm 1$, it is not clear from the numerical results whether the exact value of $M_x(0,\pm 1)$ is unbounded; cf. the discussion in [11].

Numerical solutions have been obtained for rectangular plates that are deformed by a uniform shear reaction $V = -1$ on $x = \ell$, $|y| \leq 1$ and the edges $y = \pm 1$, $0 \leq x \leq \ell$ are free. The results are qualitatively similar to those of the uniformly loaded cantilever shown in Figures 2-4. The values of $M_x(0,0)$ are given in Table III.

Table III. Rectangular Plates with $p \equiv 0$ and $V = -1$ on $x = \ell$.

ℓ	δ	$M_x(0,0)$	$M_x^i(0)$	% error
1	1/20	1.057	1	-5.39
2	1/10	2.220	2	-9.91
2	1/20	2.219	2	-9.87
4	1/10	4.644	4	-13.87

Thus $M_x^1(0)$ provides an underestimate. The accuracy of the estimate increases as δ decreases. The corresponding estimates provided by $M_x^1(\delta)$ are more accurate for the uniformly loaded rectangular cantilevers; see Table I.

The square plate with B' free is subjected to a local surface pressure p given by

$$p = \begin{cases} 1 , & |x-x'|, |y-y'| \leq \delta/2 , \\ 0 , & |x-x'|, |y-y'| > \delta/2 . \end{cases} \tag{2}$$

Since $\delta = 1/13$, the total force produced by the pressure (2) is $F = \delta^2 = 1/169$. Representative moments obtained from the computations with $x' = 23/13$, $y' = -11/13$ are shown in Figures 5. The maximum moment is $M_x(24/13,-1) = 2.304 \times 10^{-3}$. Since the solution is significantly unsymmetric, (1) is an inaccurate approximation. The reduced moment m is defined by,

$$m = \max_R M_x(x,y) \Big/ \iint_R p \, dxdy . \tag{3}$$

It relates the maximum moment to the total applied force. Let m^0 and m' denote the values of m respectively for the uniform pressure and the pressure (2). Then the stress concentration factor m'/m^0 is numerically determined as,

$$m'/m^0 = .7295 . \tag{4}$$

The swept back cantilever plate shown in Figure 1 is clamped on $x = 0$, $0 \leq y \leq 1$ and B' is free. Representative results for the uniformly loaded plate $p \equiv 1$ are shown in Figures 6. The values of $M_x(x,1/26)$ obtained with the meshes $\delta = 1/26$ and $\delta = 1/52$ are extremely close for $x > .2$. Near $x = 0$ they are considerably different. This is presumably caused by the singularity at $x = y = 0$. It is not clear whether $M_x(0,0)$ is bounded as $\delta \to 0$. The values of $M_x(x,1/26)$ obtained with the $\delta = 1/26$ mesh are in qualitative agreement with the corresponding results for square plate; see Figure 2a. The values of $M_x(x,1/2)$ obtained with the two meshes are within the resolution of the graph in Figure 6a. Since the swept back plate is geometrically unsymmetric $M_{xy}(x,1/2) \neq 0$. However, the twisting moment is generally much smaller than the other moments and is not shown in the graphs.

The rapid variation of $M_x(0,y)$ near $y = 0$ as δ decreases is presumably a result of the singularity at the corner. The maximum moment is $|M_x(0,6/52)| \approx .406$. The maximum values of $|M_x(0,y)|$ obtained with the two meshes and from (1) are summarized in Table IV.

Table IV. Maximum Moment, Uniformly Loaded Swept Plate.

δ	$\max_{0 \leq y \leq 1} \lvert M_x(0,y) \rvert$	$M_x^i(0)$	% error
1/26	.393	.5	27.2
1/52	.406	.5	23.2

The maximum occurs near $y = 0$ since a greater force is exerted by the pressure near the bottom than the top $y = 1$ of the plate. The infinite strip cantilever therefore inaccurately predicts the moments at $x = 0$. Let m_s^0 denote the value of m (3) for the uniformly loaded swept back plate. Then the numerically determined stress concentration factor

$$m_s^0/m^0 = 1.32 \tag{5}$$

occurs when the swept back plate is required to support the same total load as the square plate. Since the maximum moment for uniformly loaded rectangular plates can be reasonably approximated by $M_x^i(0)$, see Table I, it is of interest to determine the variation of the stress concentration with, the angle of sweep, the aspect ratio and the quantity a; see Figure 1. We have not conducted any calculations to estimate these variations.

$M_x(0,y)$ for the swept back plate with the pressure (2) with $\delta = 1/26$ and $x' = 23/26$, $y' = 1/13$ is shown in Figure 7. The results for the swept back plate and the square plate with the same load are qualitatively similar. The values of $M_x(0,y)$ for the square plate with the pressure (2) and the swept back plate with a uniform pressure that gives the same total force as (2) are also shown in Figure 7. This gives an indication of the stress concentration produced by localized loads and sweep back. Let m_s' denote the value of m for the swept back plate with the local pressure. Then

$$m_s'/m_s^0 = 2.89 , \quad m_s'/m' = 1.313 . \tag{6}$$

The factors in (4), (5) and (6) suggest that the combined effects of sweep back and load concentration are significantly greater than each separate effect.

The last problem discussed is the swept back plate with the data

$$V = 0 , \quad p(x,y) = y . \tag{7}$$

The maximum moment on the clamped edge is shown in Figure 8. The ratio M_{xy}/M_x is usually smaller for the load (7) than for the uniformly loaded plate. Let m_s^{ℓ} denote the value of m with the pressure (7). Then

$$m_s^0/m_s^{\ell} = 1.75 . \tag{8}$$

This happens because the larger magnitudes of p in (7) act over a smaller area and hence (7) exerts a smaller moment at x = 0. Therefore we also expect $M_x(0,y)$ to be more symmetrical about the mid-line y = 1/2; see Figures 6b and 8.

References

1. Timoshenko, S. and Woinowsky-Krieger, S., Theory of Plates and Shells, 2nd ed., McGraw-Hill, New York, 1940.

2. Southwell, R. V., "On the Analogues Relating Flexure and Extension of Flat Plates," Quarterly Journal of Mechanics and Applied Mathematics, Vol. 3, 1950, pp. 257-270.

3. Nash, W. A., "Several Approximate Analyses of the Bending of a Rectangular Cantilever Plate by Uniform Normal Pressure," Journal of Applied Mechanics, Vol. 19, 1952, pp. 33-36.

4. Sokolnikoff, I. S., Mathematical Theory of Elasticity, 2nd ed., McGraw-Hill, New York, 1956.

5. Fung, Y. C., "Bending of Thin Elastic Plates of Variable Thickness," Journal of the Aeronautical Sciences, Vol. 20, 1953, pp. 455-468.

6. Keller, H. B. and Reiss, E. L., "Iterative Solutions for the Nonlinear Bending of Circular Plates," Communications on Pure and Applied Mathematics, Vol. 9, 1958, pp. 273-292.

7. Bauer, L. and Reiss, E. L., "Nonlinear Buckling of Rectangular Plates," Journal of the Society of Industrial and Applied Mathematics, Vol. 13, 1965, pp. 603-626.

8. Bauer, F., Bauer, L., Becker, W. and Reiss, E. L., "Bending of Rectangular Plates with Finite Deflections," Journal of Applied Mechanics, Vol. 32, 1965, pp. 821-825.

9. Schechter, S., "Quasi-Tridiagonal Matrices and Type-Insensitive Difference Equations," Quarterly of Applied Mathematics, Vol. 18, 1960, pp. 285-295.

10. Bauer, F. and Reiss, E. L., "On the Numerical Determination of Shrinkage Stresses," Report Number IMM 371, Courant Institute of Mathematical Sciences, New York University, Sept. 1968.

11. Koiter, W. T. and Alblas, J. B., "On the Bending of Cantilever, Rectangular Plates," Proceedings Akad. van Wetenschappen Amsterdam, Series B, Vol. 57, 1954, pp. 250-285, 259-269, 549-557.

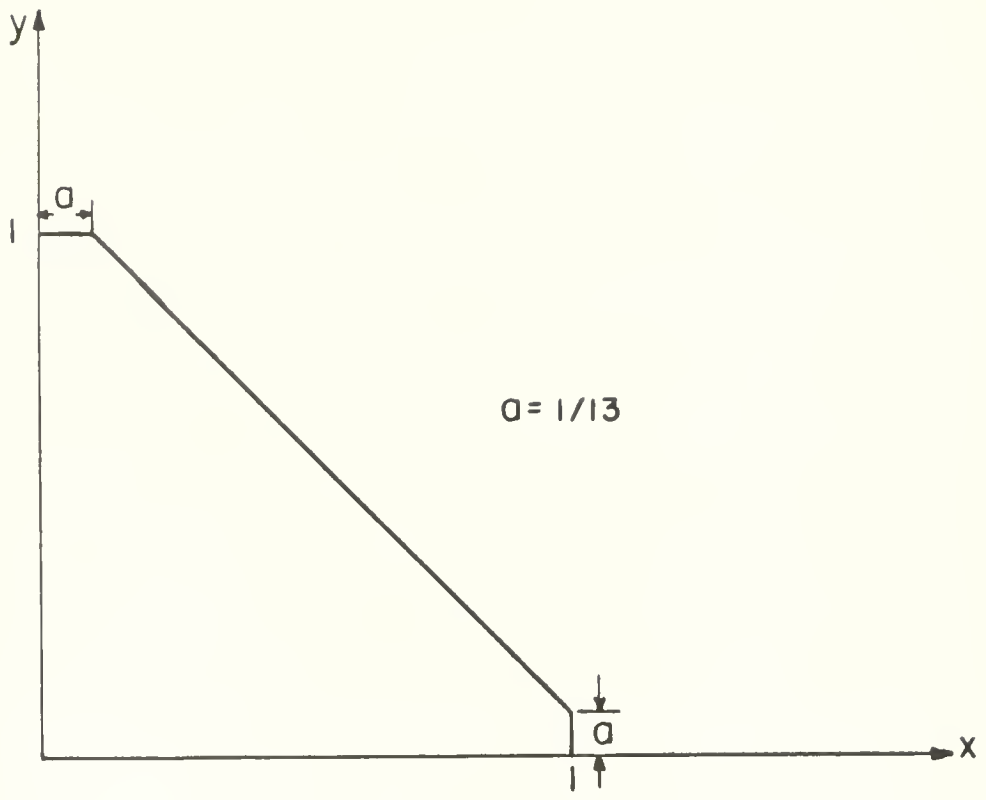

Figure 1

Sketch of Swept Back Plate.

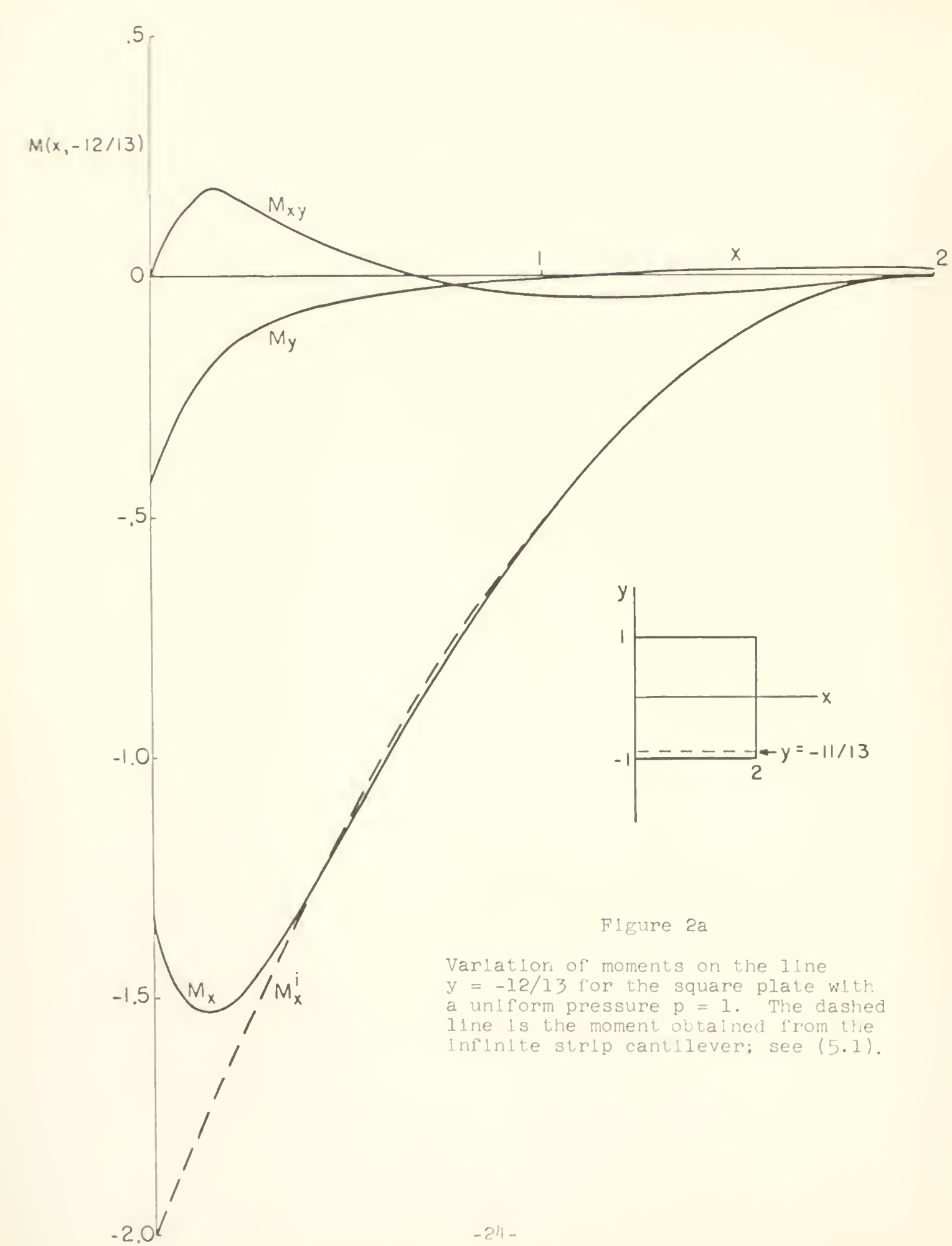

Figure 2a

Variation of moments on the line $y = -12/13$ for the square plate with a uniform pressure $p = 1$. The dashed line is the moment obtained from the infinite strip cantilever; see (5.1).

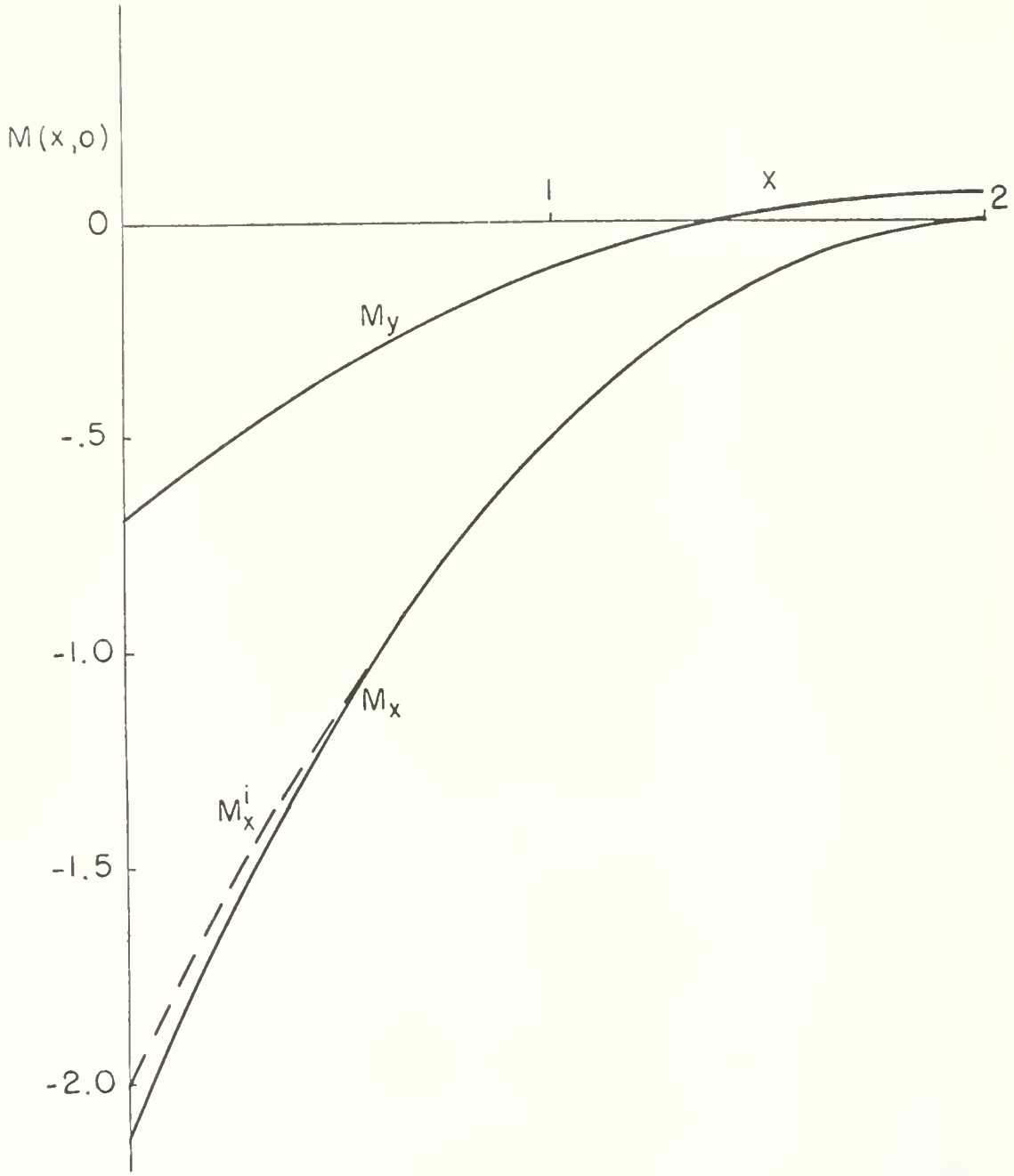

Figure 2b

Variation of moments on the center line y = 0 for the square plate with a uniform pressure p = 1.

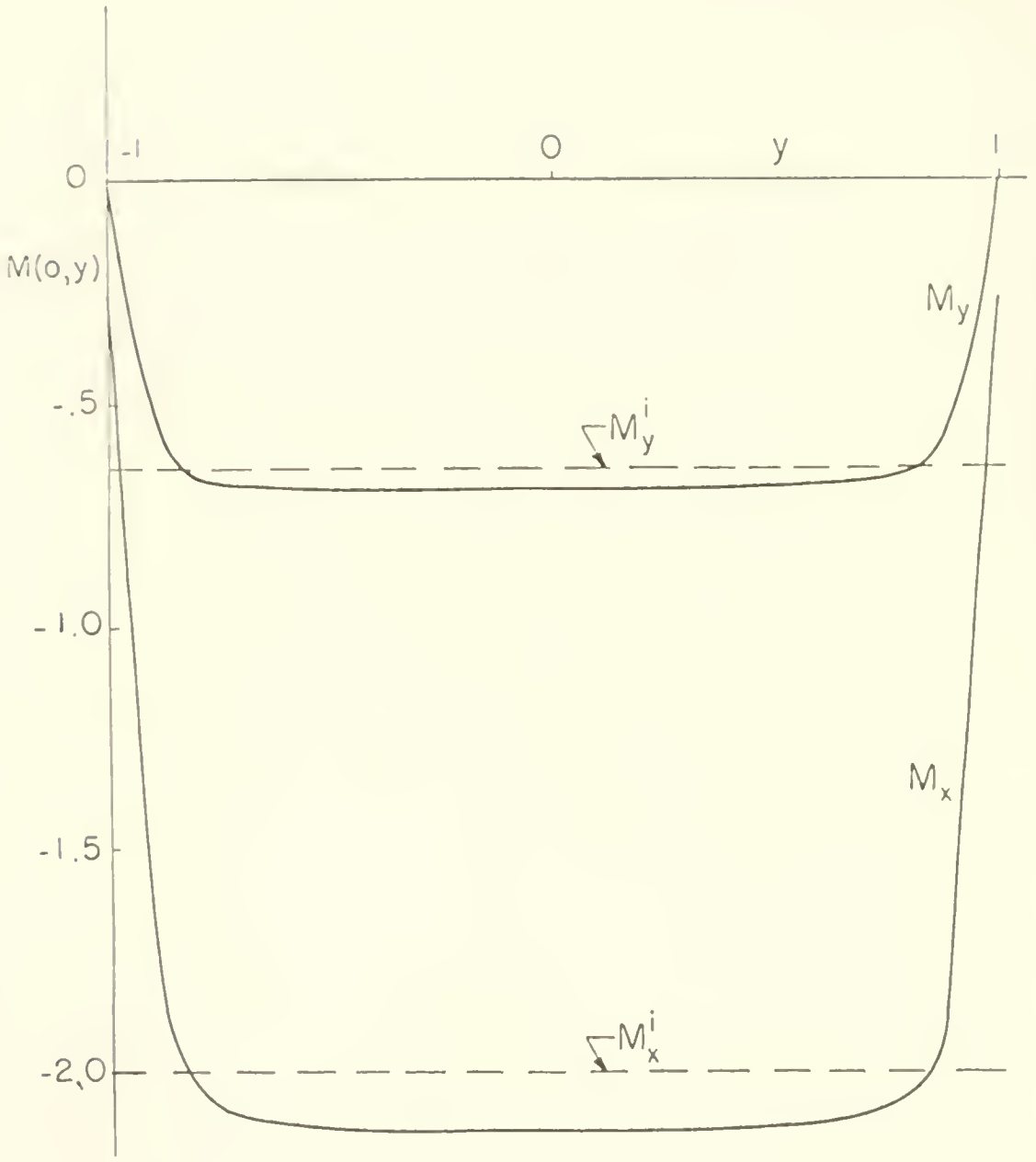

Figure 3

Variation of moments on the clamped edge, x = 0, for the square plate with a uniform pressure p = 1.

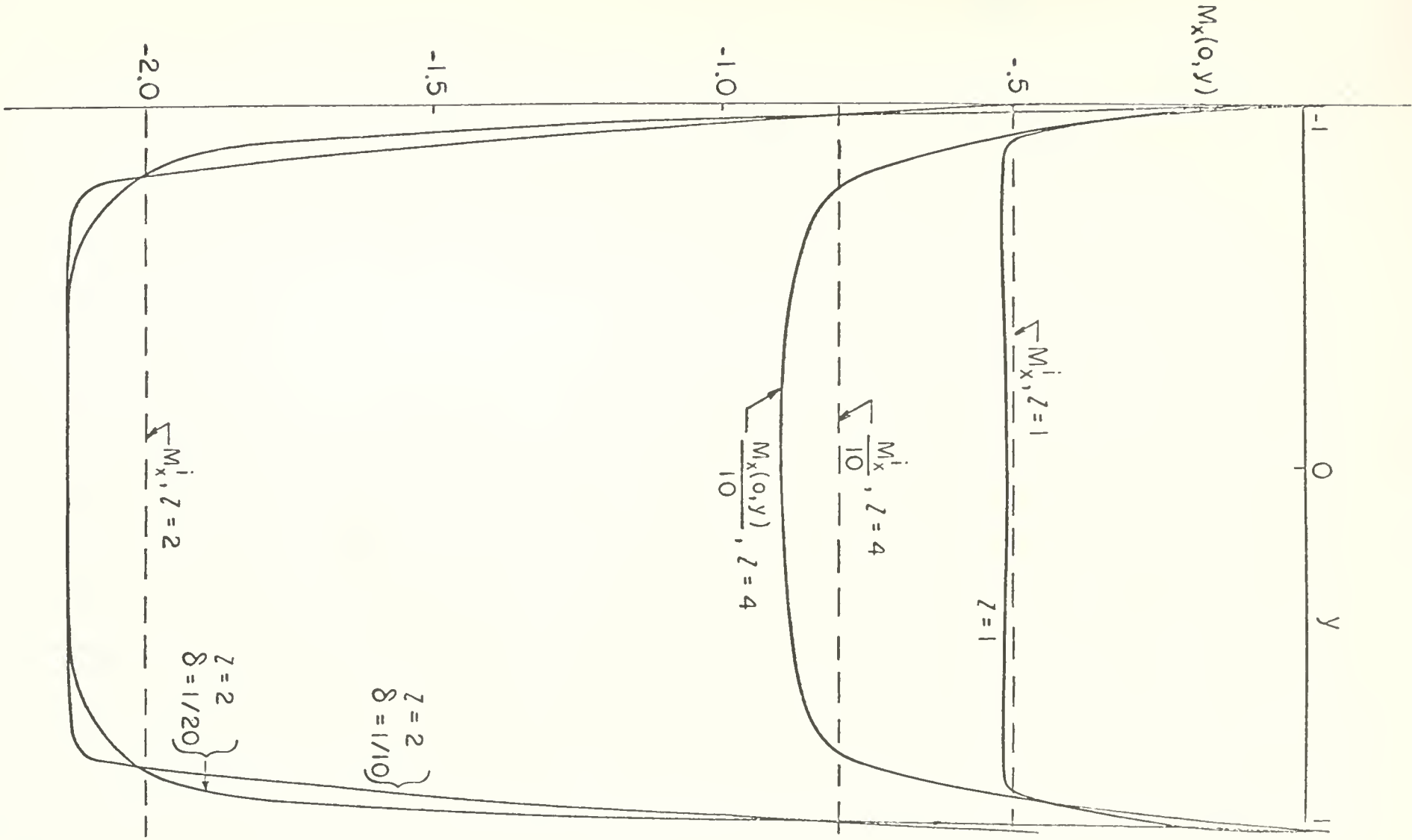

Figure 4

Variation of M_x on the clamped edge, x = 0, for the rectangular plates with a uniform pressure p = 1. For the square plate the results for two different mesh widths, $\delta = 1/10$ and $\delta = 1/20$ are shown. The maximum values of M_y on the clamped edge are: - .1659 for $\ell = 1$; - .6834 for $\ell = 2$; - 2.870 for $\ell = 4$.

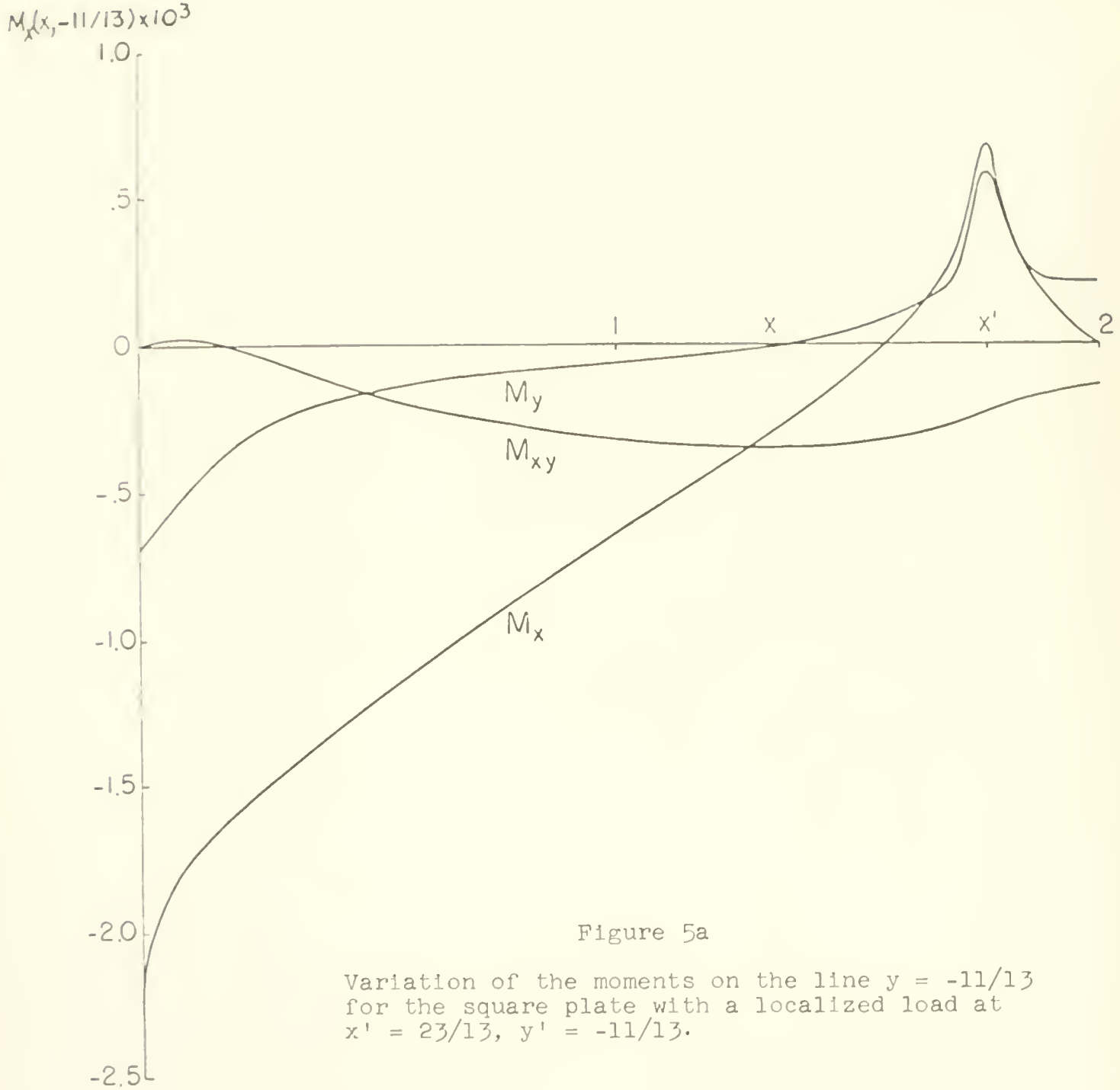

Figure 5a

Variation of the moments on the line y = -11/13 for the square plate with a localized load at x' = 23/13, y' = -11/13.

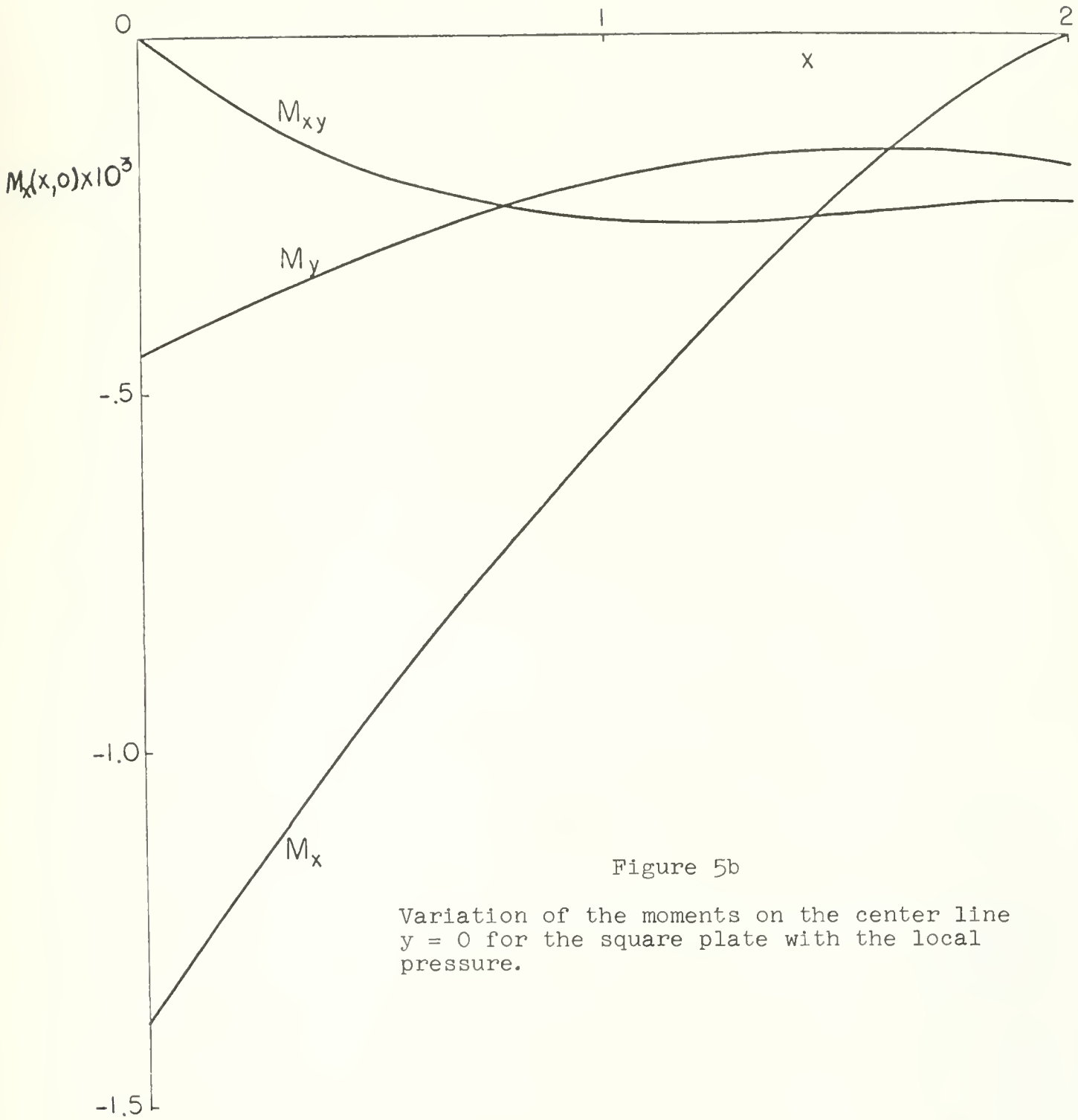

Figure 5b

Variation of the moments on the center line y = 0 for the square plate with the local pressure.

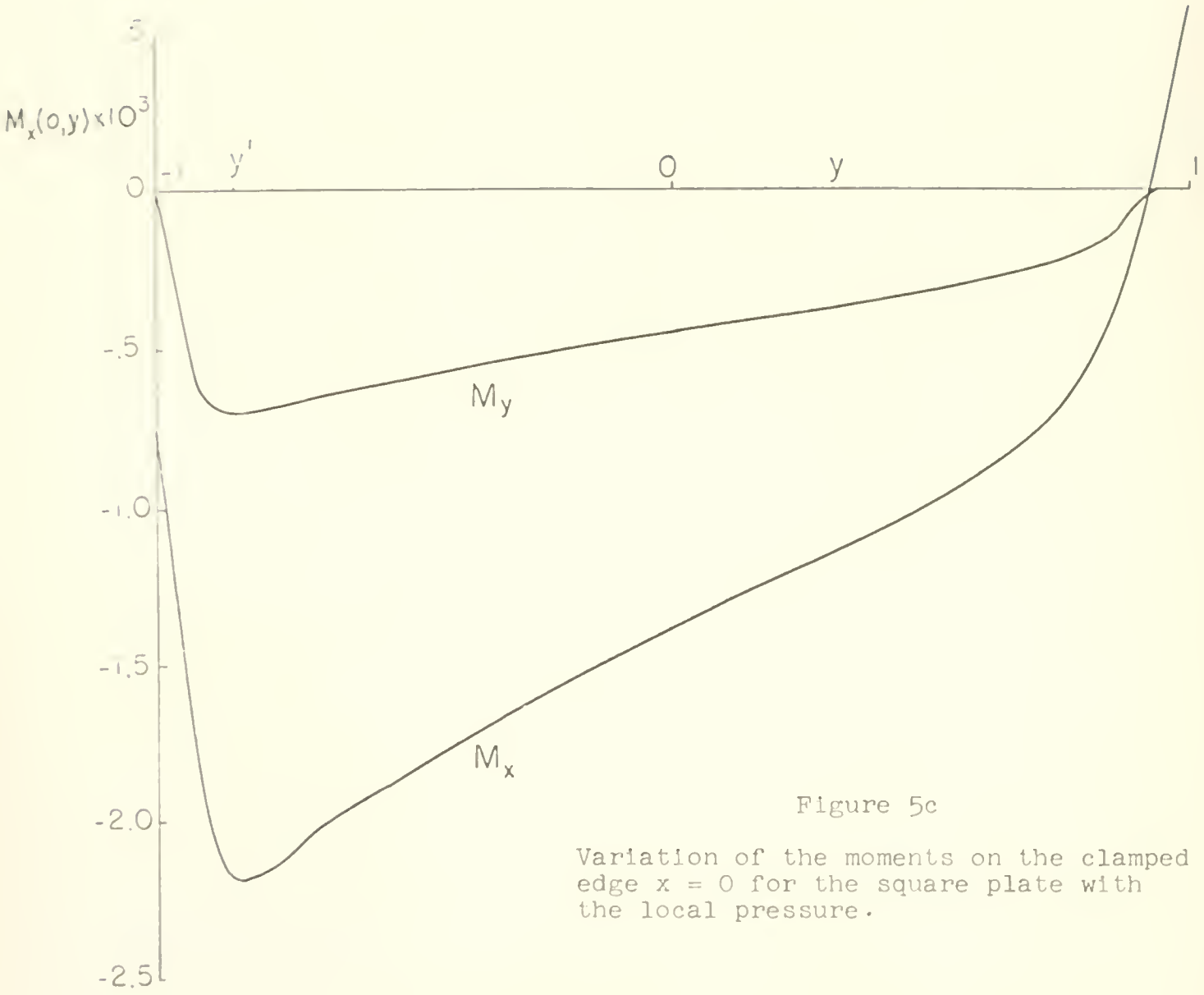

Figure 5c

Variation of the moments on the clamped edge x = 0 for the square plate with the local pressure.

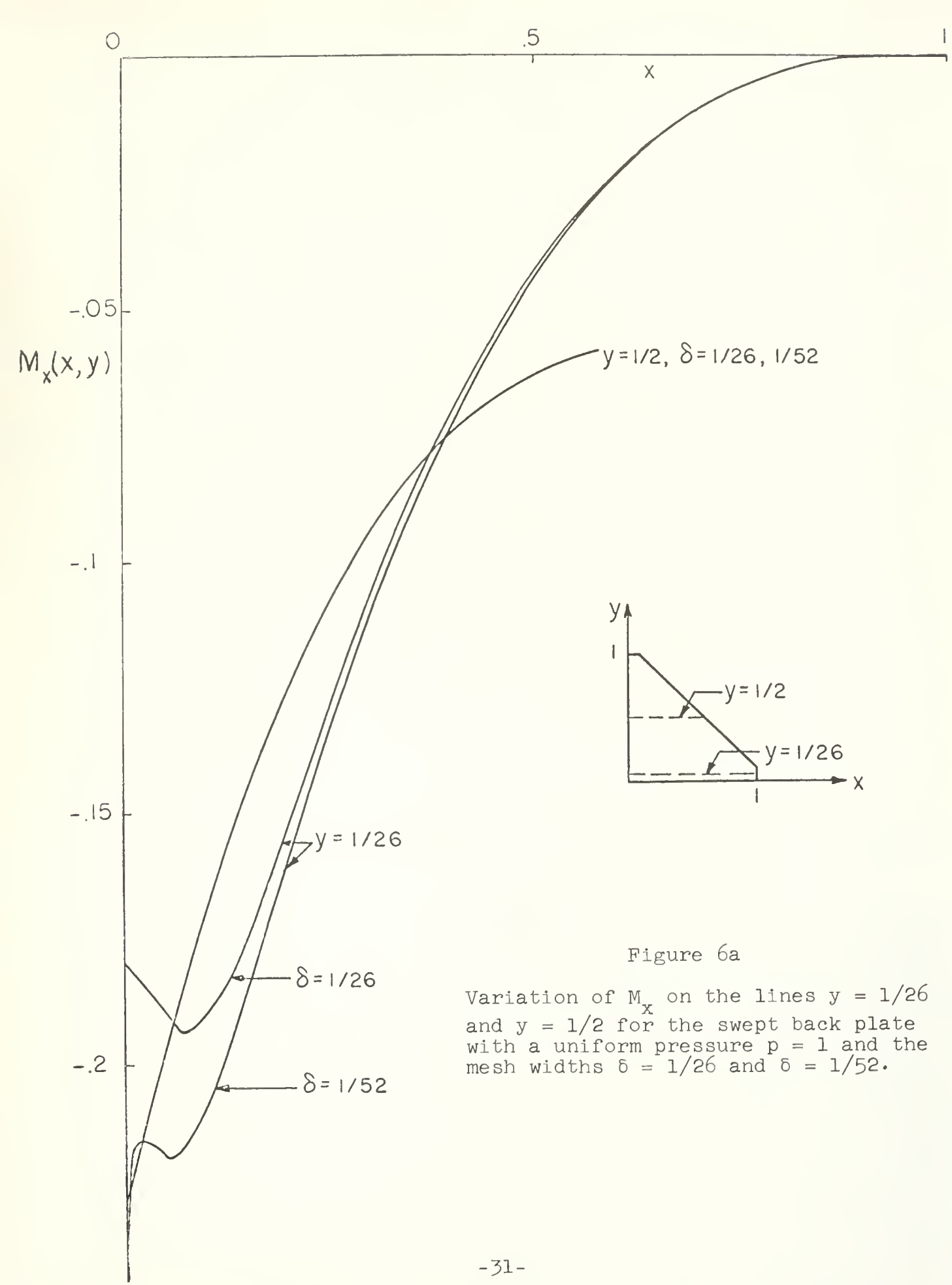

Figure 6a

Variation of M_x on the lines y = 1/26 and y = 1/2 for the swept back plate with a uniform pressure p = 1 and the mesh widths δ = 1/26 and δ = 1/52.

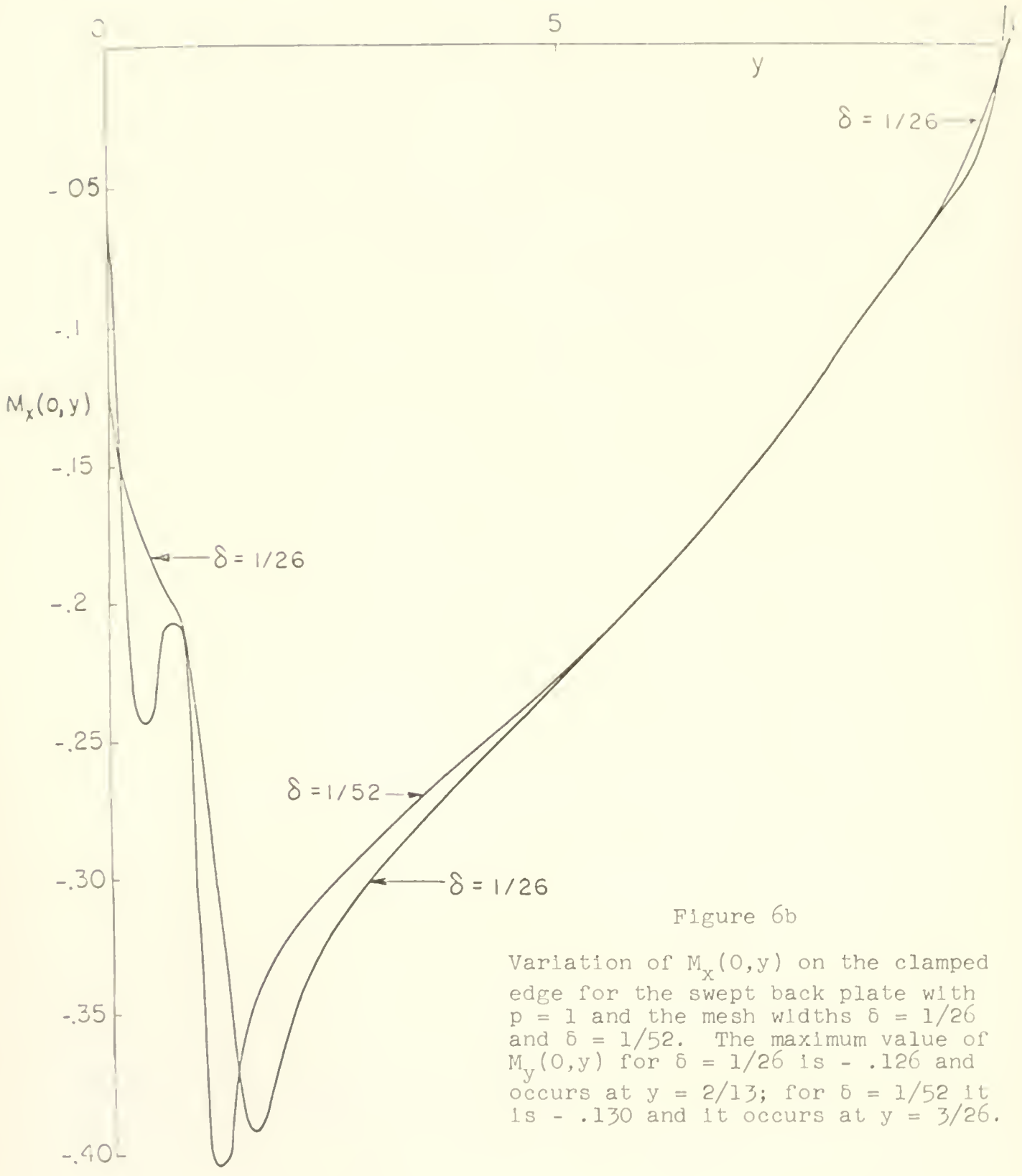

Figure 6b

Variation of $M_x(0,y)$ on the clamped edge for the swept back plate with $p = 1$ and the mesh widths $\delta = 1/26$ and $\delta = 1/52$. The maximum value of $M_y(0,y)$ for $\delta = 1/26$ is - .126 and occurs at $y = 2/13$; for $\delta = 1/52$ it is - .130 and it occurs at $y = 3/26$.

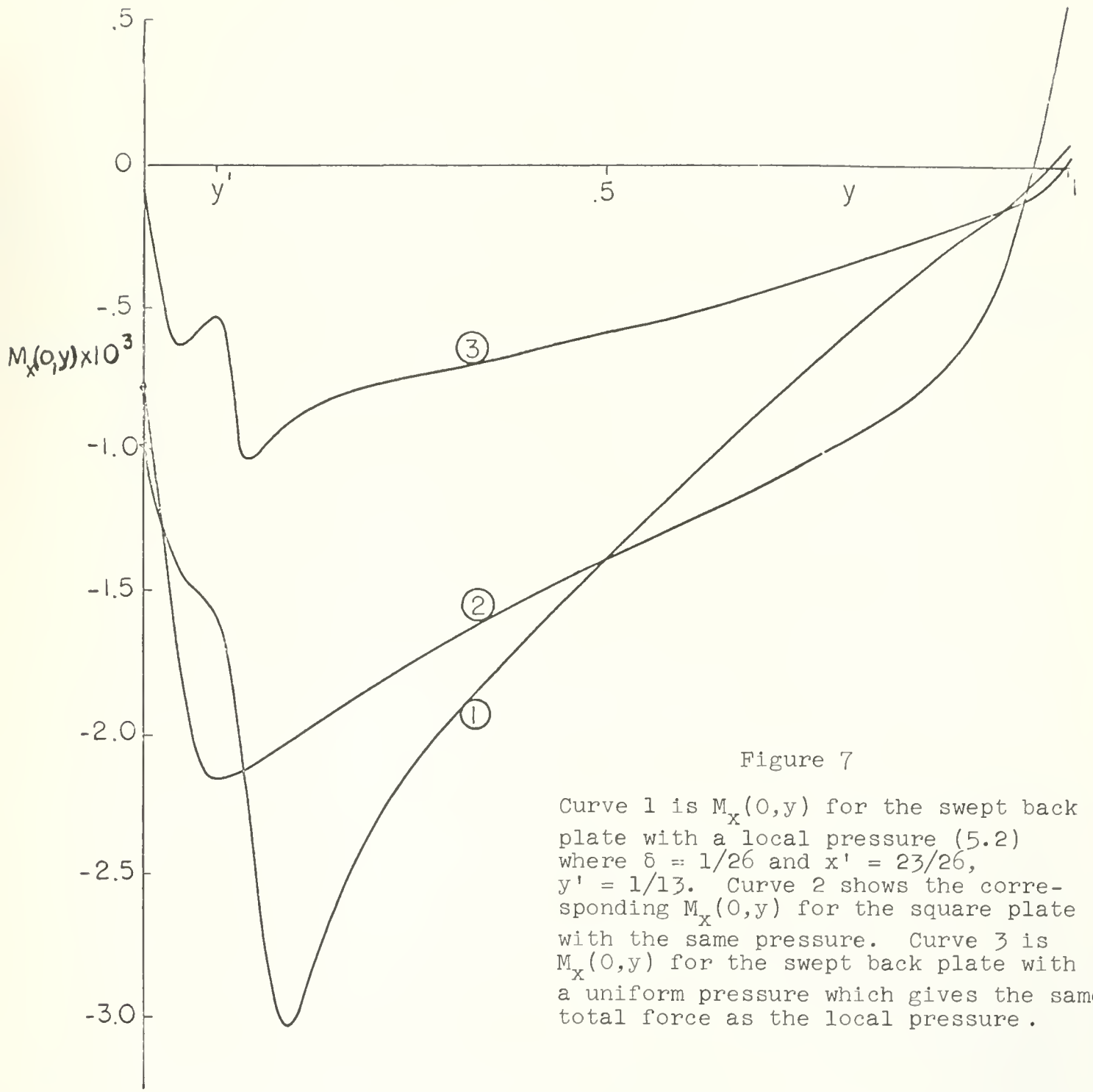

Figure 7

Curve 1 is $M_x(0,y)$ for the swept back plate with a local pressure (5.2) where $\delta = 1/26$ and $x' = 23/26$, $y' = 1/13$. Curve 2 shows the corresponding $M_x(0,y)$ for the square plate with the same pressure. Curve 3 is $M_x(0,y)$ for the swept back plate with a uniform pressure which gives the same total force as the local pressure.

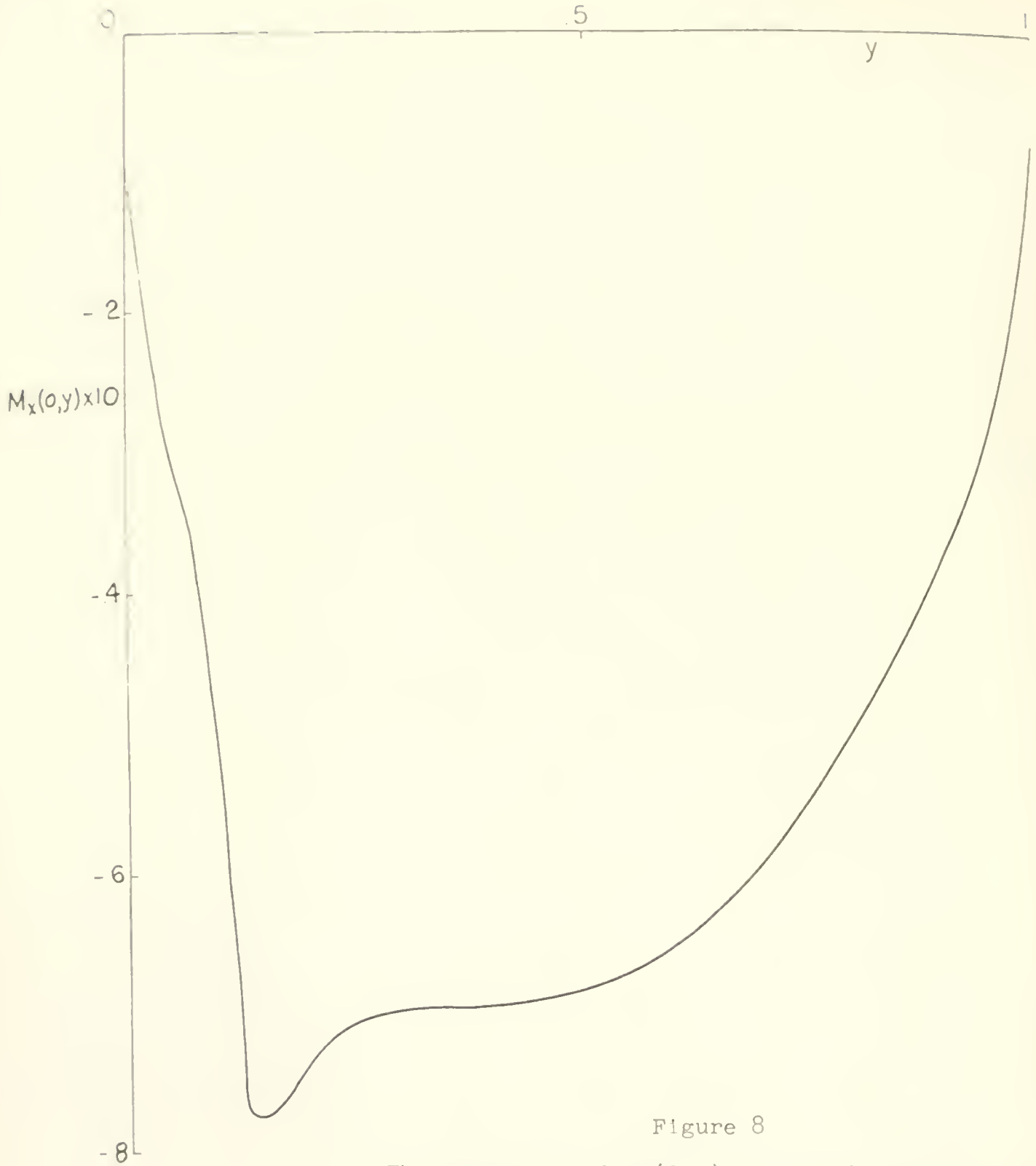

Figure 8

The variation of $M_x(0,y)$ on the clamped edge for the swept back plate with the linear pressure distribution (5.7). The graph of $M_y(0,y)$ is similar to the one for $M_x(0,y)$ but with small magnitude. The maximum value of $M_y(0,y) = -.02477$ and occurs at $y = 2/13$.

Security Classification

DOCUMENT CONTROL DATA - R&D

(Security classification of title, body of abstract and indexing annotation must be entered when the overall report is classified)

1. ORIGINATING ACTIVITY (Corporate author) Courant Institute of Mathematical Sciences New York University	2a. REPORT SECURITY CLASSIFICATION not classified 2b GROUP none

3 REPORT TITLE

Stresses in Cantilever Plates

4 DESCRIPTIVE NOTES (Type of report and inclusive dates)

Technical Report February 1969

5. AUTHOR(S) (Last name, first name, initial)

Bauer, Frances and Reiss, Edward L.

6. REPORT DATE	7a. TOTAL NO. OF PAGES	7b. NO. OF REFS
February 1969	34	11

8a. CONTRACT OR GRANT NO. Nonr-285(42) b. PROJECT NO. NR 064-438 c. d.	9a. ORIGINATOR'S REPORT NUMBER(S) IMM 374 9b. OTHER REPORT NO(S) (Any other numbers that may be assigned this report) none

10. AVAILABILITY/LIMITATION NOTICES

Distribution of this document is unlimited.

11. SUPPLEMENTARY NOTES none	12. SPONSORING MILITARY ACTIVITY U.S. Navy, Office of Naval Research 207 West 24th St., New York, N.Y.

13. ABSTRACT

Key Words: Cantilever Plates, Numerical Methods, Plates.

A numerical method is presented for determining the bending stresses in elastic cantilever plates. Southwell's formulation of the classical small deflection plate theory is employed. The method is applied to obtain numerical solutions for rectangular and swept back plates subjected to a variety of surface and edge loads. Boundary layer effects are observed for the uniformly loaded rectangular plates as the length of the plate decreases. The effects of a load concentration and sweep back are observed and summarized in the form of stress concentration factors.

DD FORM 1 JAN 64 1473

Security Classification

14 KEY WORDS	LINK A		LINK B		LINK C	
	ROLE	WT	ROLE	WT	ROLE	WT

INSTRUCTIONS

1. ORIGINATING ACTIVITY: Enter the name and address of the contractor, subcontractor, grantee, Department of Defense activity or other organization *(corporate author)* issuing the report.

2a. REPORT SECURITY CLASSIFICATION: Enter the overall security classification of the report. Indicate whether "Restricted Data" is included. Marking is to be in accordance with appropriate security regulations.

2b. GROUP: Automatic downgrading is specified in DoD Directive 5200.10 and Armed Forces Industrial Manual. Enter the group number. Also, when applicable, show that optional markings have been used for Group 3 and Group 4 as authorized.

3. REPORT TITLE: Enter the complete report title in all capital letters. Titles in all cases should be unclassified. If a meaningful title cannot be selected without classification, show title classification in all capitals in parenthesis immediately following the title.

4. DESCRIPTIVE NOTES: If appropriate, enter the type of report, e.g., interim, progress, summary, annual, or final. Give the inclusive dates when a specific reporting period is covered.

5. AUTHOR(S): Enter the name(s) of author(s) as shown on or in the report. Enter last name, first name, middle initial. If military, show rank and branch of service. The name of the principal author is an absolute minimum requirement.

6. REPORT DATE: Enter the date of the report as day, month, year, or month, year. If more than one date appears on the report, use date of publication.

7a. TOTAL NUMBER OF PAGES: The total page count should follow normal pagination procedures, i.e., enter the number of pages containing information.

7b. NUMBER OF REFERENCES: Enter the total number of references cited in the report.

8a. CONTRACT OR GRANT NUMBER: If appropriate, enter the applicable number of the contract or grant under which the report was written.

8b, 8c, & 8d. PROJECT NUMBER: Enter the appropriate military department identification, such as project number, subproject number, system numbers, task number, etc.

9a. ORIGINATOR'S REPORT NUMBER(S): Enter the official report number by which the document will be identified and controlled by the originating activity. This number must be unique to this report.

9b. OTHER REPORT NUMBER(S): If the report has been assigned any other report numbers *(either by the originator or by the sponsor)*, also enter this number(s).

10. AVAILABILITY/LIMITATION NOTICES: Enter any limitations on further dissemination of the report, other than those imposed by security classification, using standard statements such as:

(1) "Qualified requesters may obtain copies of this report from DDC."

(2) "Foreign announcement and dissemination of this report by DDC is not authorized."

(3) "U. S. Government agencies may obtain copies of this report directly from DDC. Other qualified DDC users shall request through

_____."

(4) "U. S. military agencies may obtain copies of this report directly from DDC. Other qualified users shall request through

_____."

(5) "All distribution of this report is controlled. Qualified DDC users shall request through

_____."

If the report has been furnished to the Office of Technical Services, Department of Commerce, for sale to the public, indicate this fact and enter the price, if known.

11. SUPPLEMENTARY NOTES: Use for additional explanatory notes.

12. SPONSORING MILITARY ACTIVITY: Enter the name of the departmental project office or laboratory sponsoring *(paying for)* the research and development. Include address.

13. ABSTRACT: Enter an abstract giving a brief and factual summary of the document indicative of the report, even though it may also appear elsewhere in the body of the technical report. If additional space is required, a continuation sheet shall be attached.

It is highly desirable that the abstract of classified reports be unclassified. Each paragraph of the abstract shall end with an indication of the military security classification of the information in the paragraph, represented as *(TS)*, *(S)*, *(C)* or *(U)*.

There is no limitation on the length of the abstract. However, the suggested length is from 150 to 225 words.

14. KEY WORDS: Key words are technically meaningful terms or short phrases that characterize a report and may be used as index entries for cataloging the report. Key words must be selected so that no security classification is required. Identifiers, such as equipment model designation, trade name, military project code name, geographic location, may be used as key words but will be followed by an indication of technical context. The assignment of links, roles, and weights is optional.

DISTRIBUTION LIST - Nonr-285(42)

PART I - GOVERNMENT

Administrative & Liaison Activities

Chief of Naval Research
Attn:
Code 423
439 (2)
468
Department of the Navy
Washington, D. C. 20360

Commanding Officer
ONR Branch Office
495 Summer Street
Boston, Massachusetts 02210

Commanding Officer
ONR Branch Office
219 S. Dearborn Street
Chicago, Illinois 60604

Commanding Officer
ONR Branch Office
Box 39, Navy 100
c/o Fleet Post Office
New York, New York 09510 (5)

New York Area Office
Scientific Department
Office of Naval Research
207 West 24th Street
New York, New York 10011

Commanding Officer
ONR Branch Office
1030 E. Green Street
Pasadena, California 91101

Commanding Officer
ONR Branch Office
U.S. Post Office & Courts Bldg.
1076 Mission Street
San Francisco, California 94103

U. S. Naval Research Laboratory
Attn: Technical Information Div.
Washington, D. C. 20390 (6)

Defense Documentation Center
Cameron Station
Alexandria, Virginia 22314 (20)

Office of Naval Research
495 Summer Street
Boston, Mass. 02210

Army

Commanding Officer
U. S. Army Research Off.-Durham
Attn: Mr. J. J. Murray
CRD-AA-IP
Box CM, Duke Station
Durham, North Carolina 27706

Commanding Officer
AMXMR-ATL
U. S. Army Materials Res. Agcy.
Watertown, Massachusetts 02172

Redstone Scientific Info. Center
Chief, Document Section
U. S. Army Missile Command
Redstone Arsenal, Alabama 35809

AMSMI-RKP
Attn: Mr. T. H. Duerr
Redstone Arsenal, Alabama 35809

Ballistic Research Laboratories
Attn: Dr. A. S. Elder
Aberdeen Proving Ground
Aberdeen, Maryland 21005

Ballistic Research Laboratories
Attn: Mr. H. P. Gay
AMXBR-ID
Aberdeen Proving Ground
Aberdeen, Maryland 21005

Technical Library
Aberdeen Proving Ground
Aberdeen, Maryland 21005

Navy

Commanding Officer and Director
Attn: Code 042 (Cent. Lib. Br.)
050
700 (Struc. Mech. Lab.)
720
725
740 (Mr. W. J. Sette)
901 (Dr. M. Strassberg)
941 (Dr. R. Liebowitz)
945 (Mr. A. O. Sykes)
960 (Mr. E. F. Noonan)
962 (Dr. E. Buchmann)
David Taylor Model Basin
Washington, D. C. 20007

Mr. Garet A. Bornstein
U. S. Naval Propellant Plant
Indian Head, Maryland 20640

Undersea Explosion Research Div.
Attn: Mr. D. S. Cohen
Code 750
David Taylor Model Basin
Norfolk Naval Shipyard
Portsmouth, Virginia 23709

Commanding Officer & Director
Code 257, Library
U. S. Navy Marine Engr. Lab.
Annapolis, Maryland 21402

Commander
Technical Library
U. S. Naval Ordnance Test Station
Pasadena Annex
3202 E. Foothill Blvd.
Pasadena, California 91107

U. S. Naval Ordnance Test Station
Attn: Dr. Arnold Adicoff
Code 5056
China Lake, California 93557

Commander
U. S. Naval Ordnance Test Station
Mechanical Engineering Division
Code 556
China Lake, California 93557

Commanding Officer & Director
U. S. Naval Civil Engr. Lab.
Code L31
Port Hueneme, California 93041

Shipyard Technical Library
Code 242L
Portsmouth Naval Shipyard
Portsmouth, New Hampshire 03804

U. S. Naval Electronics Laboratory
Attn: Dr. R. J. Christensen
San Diego, California 92152

U. S. Naval Ordnance Laboratory
Mechanics Division
RFD 1, White Oak
Silver Spring, Maryland 20910

U. S. Naval Ordnance Laboratory
Attn: Mr. H. A. Perry, Jr.
Non-Metallic Materials Division
Silver Spring, Maryland 20910

Supervisor of Shipbuilding
U. S. Navy
Newport News, Virginia 23607

Shipyard Technical Library
Building 746, Code 303TL
Mare Island Naval Shipyard
Vallejo, California 94592

Director
U.S. Navy Underwater Sound Ref. Lab.
Office of Naval Research
P. O. Box 8337
Orlando, Florida 32806

Technical Library
U. S. Naval Propellant Plant
Indian Head, Maryland 20640

U. S. Naval Propellant Plant
Attn: Dr. J. G. Tuono
Research & Development Division
Indian Head, Maryland 20640

Chief of Naval Operations
Attn: Code Op-03EG
Op-07T
Department of the Navy
Washington, D. C. 20350

Director, Special Projects
Attn: Sp-001
43
2731
Department of the Navy
Washington, D. C. 20360

Executive Secretary PLRRD
Special Projects Office (Sp-00110)
Department of the Navy
Washington, D. C. 20360

U. S. Naval Applied Science Lab.
Code 9832
Technical Library
Building 291, Naval Base
Brooklyn, New York 11251

Director
Aeronautical Materials Lab.
Naval Air Engineering Center
Naval Base
Philadelphia, Pennsylvania 19112

Navy (cont'd.)

Director
Aeronautical Structures Lab.
Naval Air Engineering Center
Naval Base
Philadelphia, Pennsylvania 19112

Director
Attn: Code 5360
5500
6200
6210
6250
6260
Technical Library
Naval Research Laboratory
Washington, D. C. 20390

Chief, Bureau of Naval Weapons
Attn: Code DLI-3
R-12
RAAD-2
RAAD-24 (Mr. E.M. Ryan)
RM
RMMP-2
RMMP-11 (Mr. I. Silver)
RMMP-22 (Mr. J.C. Ardinger)
RR
RRRE
RRRE-61 (Mr. W.J. Marciniak)
RU
Department of the Navy
Washington, D. C. 20360

Chief, Bureau of Ships
Attn: Code 210-L
305
345
421
423
430
440
442
443
1500
Department of the Navy
Washington, D. C. 20360

Commander
U. S. Naval Weapons Laboratory
Dahlgren, Virginia 22448

Mr. Ernest A. Hogge
Head, Scientific Support Division
U. S. Navy Mine Defense Laboratory
Panama City, Florida 32402

Bureau of Yards & Docks Tech. Lib.
Yards & Docks Annex
Department of the Navy
Washington, D. C. 20390

Air Force

Commander, WADD
Attn: Code WWRMDD
AFFDL (FDDS)
Structures Division
AFLC (MCEEA)
Code WWRMDS
AFFDL (FDT)
Code WWRC
AFML (MAAM)
Code WCLSY
SEG (SEFSD, Mr. Lakin)
Wright-Patterson Air Force Base
Dayton, Ohio 45433

Commander
Chief, Applied Mechanics Group
U. S. Air Force Inst. of Tech.
Wright-Patterson Air Force Base
Dayton, Ohio 45433

Chief, Civil Engineering Branch
WLRC, Research Division
Air Force Weapons Laboratory
Kirtland AFB, New Mexico 87117

Commander
AFRPL (RPMC/Dr. F.N. Kelley)
Edwards AFB, California 93523

Commander
Attn: Mr. A.L. Skinner, OOMQQC
Hill AFB, Utah 84401

Commander
Mechanics Division
Air Force Office of Scien. Res.
Washington, D. C. 20333

NASA

Structures Research Division
Attn: Mr. R. R. Heldenfels, Chief
National Aeronautics & Space Admin.
Langley Research Center
Langley Station
Hampton, Virginia 23365

NASA (cont'd.)

National Aeronautics & Space Admin.
Code RV-2
Washington, D. C. 20546

National Aeronautics & Space Admin.
Associate Administrator for Advanced
Research & Technology
Washington, D. C. 20546

Scientific & Tech. Info. Facility
NASA Representative (S-AK/DL)
P. O. Box 5700
Bethesda, Maryland 20014

Other Government Activities

Commandant
Chief, Testing & Development Div.
U. S. Coast Guard
1300 E Street, N. W.
Washington, D. C. 20226

Director
Marine Corps Landing Force Devel. Cen.
Marine Corps Schools
Quantico, Virginia 22134

Director
Attn: Mr. B. L. Wilson
National Bureau of Standards
Washington, D. C. 20234

National Science Foundation
Engineering Division
1951 Constitution Avenue, N. W.
Washington, D. C. 20550

Science & Tech. Division
Library of Congress
Washington, D. C. 20540

Director
STBS
Defense Atomic Support Agency
Washington, D. C. 20301

Commander Field Command
Defense Atomic Support Agency
Sandia Base
Albuquerque, New Mexico 87115

Chief, Defense Atomic Support Agcy.
Blast & Shock Division
The Pentagon
Washington, D. C. 20301

Director Defense Research & Engr.
Technical Library
Room 3C-128
The Pentagon
Washington, D. C. 20301

Chief, Airframe & Equipment Branch
FS-120
Office of Flight Standards
Federal Aviation Agency
Washington, D. C. 20553

Chief, Division of Ship Design
Maritime Administration
Washington, D. C. 20235

Deputy Chief, Office of Ship Constr.
Attn: Mr. U. L. Russo
Maritime Administration
Washington, D. C. 20235

Executive Secretary
Committee on Undersea Warfare
National Academy of Sciences
2101 Constitution Avenue
Washington, D. C. 20418

Ship Hull Research Committee
Attn: Mr. A. R. Lytle
National Research Council
National Academy of Sciences
2101 Constitution Avenue
Washington, D. C. 20418

PART II - CONTRACTORS AND OTHER
TECHNICAL COLLABORATORS

Universities

Dr. D. C. Drucker
Division of Engineering
Brown University
Providence, Rhode Island 02912

Professor J. Edmund Fitzgerald
Chairman, Department of Civil
Engineering
University of Utah
Salt Lake City, Utah 84112

Universities (cont'd)

Prof. M. E. Gurtin
Brown University
Providence, Rhode Island 02912

Prof. R. S. Rivlin
Division of Applied Mathematics
Brown University
Providence, Rhode Island 02912

Prof. P. J. Blatz
Materials Science Department
California Institute of Technology
Pasadena, California 91109

Prof. Julius Miklowitz
Div. of Engr. & Applied Sciences
California Institute of Technology
Pasadena, California 91109

Prof. George Sih
Department of Mechanics
Lehigh University
Bethlehem, Pennsylvania 18015

Solid Propellant Library
Firestone Flight Science Lab.
California Institute of Technology
Pasadena, California 91109

Prof. Eli Sternberg
Div. ofEngr. & Applied Sciences
California Institute of Technology
Pasadena, California 91109

Prof. Paul M. Naghdi
Div. of Applied Mechanics
Etcheverry Hall
University of California
Berkeley, California 94720

Prof. J. Baltrukonis
Mechanics Division
The Catholic Univ. of America
Washington, D. C. 20017

Dr. Y. Weitsman
Div. of Applied Mathematics
Brown University
Providence, R.I. 02912

Prof. A. J. Durelli
Mechanics Division
The Catholic Univ. of America
Washington, D. C. 20017

Prof. H. H. Bleich
Departmentof Civil Engr.
Columbia University
Amsterdam & 120th Street
New York, New York 10027

Prof. R. D. Mindlin
Department of Civil Engr.
Columbia University
S. W. Mudd Building
New York, New York 10027

Prof. B. A. Boley
Department of Civil Engr.
Columbia University
Amsterdam & 120th Street
New York, New York 10027

Prof. F. L. DiMaggio
Department of Civil Engr.
Columbia University
616 Mudd Building
New York, New York 10027

Prof. A. M. Freudenthal
Dept. of Civil Engr. & Engr. Mech.
Columbia University
New York, New York 10027

Prof. William A. Nash
Dept. of Mechanical and Aerospace
Engineering
College of Engineering
University of Massachusetts
Amherst, Mass. 01002

Prof. B. Budiansky
Div. of Engr. & Applied Physics
Pierce Hall
Harvard University
Cambridge, Massachusetts 02138

Prof. P. G. Hodge
Department of Mechanics
Illinois Institute of Technology
Chicago, Illinois 60616

Dr. S. Dharmarajan
Head, Post Graduate Dept. of
Machine Design & Mechanics
P.S.G. College of Technology
Coimbatore, Madras State
India

Universities (cont'd)

Prof. H. T. Corten
212 Talbot Lab.
University of Illinois
Urbana, Illinois 61803

Prof. W. J. Hall
Department of Civil Engr.
University of Illinois
Urbana, Illinois 61803

Prof. N. M. Newmark
Dept. of Civil Engineering
University of Illinois
Urbana, Illinois 61803

Dr. W. H. Avery
Applied Physics Laboratory
Johns Hopkins University
8621 Georgia Avenue
Silver Spring, Maryland 20910

Prof. J. B. Tiedemann
Dept. of Aero. Engr. & Arch.
University of Kansas
Lawrence, Kansas 66045

Prof. S. Taira
Department of Engineering
Kyoto University
Kyoto, Japan

Prof. E. Reissner
Dept. of Mathematics
Massachusetts Inst. of Tech.
Cambridge, Massachusetts 02139

Library (Code 0384)
U. S. Naval Postgraduate School
Monterey, California 93940

Dr. Joseph Marin
Prof. of Materials Science
Dept. of Materials Sc. & Chem.
U. S. Naval Postgraduate School
Monterey, California 93940

Prof. E. L. Reiss
Courant Inst. of Math. Sciences
New York University
4 Washington Place
New York, New York 10003

Dr. Francis Cozzarelli
Div. of Interdisciplinary
Studies and Research
School of Engineering
State Univ. of N.Y. at Buffalo
Buffalo, New York 14214

Dr. George Herrmann
The Technological Institute
Northwestern University
Evanston, Illinois 60201

Director, Ordnance Research Lab.
The Pennsylvania State University
P. O. Box 30
State College, Pennsylvania 16801

Prof. Eugen J. Skudrzyk
Department of Physics
Ordnance Research Lab.
The Pennsylvania State University
P. O. Box 30
State College, Pennsylvania 16801

Dean Oscar Baguio
College of Engineering
University of the Philippines
Quezon City, Philippines

Prof. J. Kempner
Dept. of Aero. Engr. & Applied Mech.
Polytechnic Institute of Brooklyn
333 Jay Street
Brooklyn, New York 11201

Prof. J. Klosner
Polytechnic Institute of Brooklyn
333 Jay Street
Brooklyn, New York 11201

Prof. F. R. Eirich
Polytechnic Institute of Brooklyn
333 Jay Street
Brooklyn, New York 11201

Prof. A. C. Eringen
Aerospace & Mechanical Sciences
Princeton University
Princeton, New Jersey

Tamar Singer
Library of Exact Science
Tel Aviv University
Ramat Aviv, Tel Aviv, Israel

Universities (cont'd.)

Dr. S. L. Koh
School of Aero., Astro. & Engr. Sc.
Purdue University
Lafayette, Indiana 47907

Prof. D. Schapery
Purdue University
Lafayette, Indiana 47907

Prof. E. H. Lee
Div. of Engr. Mechanics
Stanford University
Stanford, California 94305

Dr. Nicholas J. Hoff
Dept. of Aero. & Astro.
Stanford University
Stanford, California 94305

Prof. J. N. Goodier
Div. of Engr. Mechanics
Stanford University
Stanford, California 94305

Prof. Markus Reiner
Technion R & D Foundation, Ltd.
Haifa, Israel

Prof. Tsuyoshi Hayashi
Department of Aeronautics
Faculty of Engineering
University of Tokyo
BUNKYO-KU
Tokyo, Japan

Prof. R. J. H. Bollard
Chairman, Aeronautical Engr. Dept.
207 Guggenheim Hall
University of Washington
Seattle, Washington 98105

Prof. Albert S. Kobayashi
Dept. of Mechanical Engr.
University of Washington
Seattle, Washington 98105

Officer-in-Charge
Post Graduate School for Naval Off.
Webb Institute of Naval Arch.
Crescent Beach Road, Glen Cove
Long Island, New York 11542

Industry and Research Institutes

Mr. K. W. Bills, Jr.
Dept. 4722, Bldg. 0525
Aerojet-General Corporation
P. O. Box 1947
Sacramento, California 95809

Dr. James H. Wiegand
Senior Dept. 4720, Bldg. 0525
Ballistics & Mech. Properties Lab.
Aerojet-General Corporation
P. O. Box 1947
Sacramento, California 95809

Mr. J. S. Wise
Aerospace Corporation
P. O. Box 1308
San Bernardino, California 92402

Dr. Vito Salerno
Applied Technology Assoc., Inc.
29 Church Street
Ramsey, New Jersey 07446

Library Services Department
Report Section, Bldg. 14-14
Argonne National Laboratory
9700 S. Cass Avenue
Argonne, Illinois 60440

Dr. E. M. Kerwin
Bolt, Beranek, & Newman, Inc.
50 Moulton Street
Cambridge, Massachusetts 02138

Dr. M. C. Junger
Cambridge Acoustical Associates
129 Mount Auburn Street
Cambridge, Massachusetts 02138

Dr. F. R. Schwarzl
Central Laboratory T.N.O.
134 Julianalaan
Delft, Holland

Industry & Research Inst. (cont'd.)

Mr. Ronald D. Brown
Applied Physics Laboratory
Chemical Propulsion Agency
8621 Georgia Avenue
Silver Spring, Maryland 20910

Research and Development
Electric Boat Division
General Dynamics Corporation
Groton, Connecticut 06340

Supervisor of Shipbuilding, USN,
and Naval Insp. of Ordnance
Electric Boat Division
General Dynamics Corporation
Groton, Connecticut 06340

Dr. L. H. Chen
Basic Engineering
Electric Boat Division
General Dynamics Corporation
Groton, Connecticut 06340

Mr. Ross H. Petty
Technical Librarian
Allegany Ballistics Lab.
Hercules Powder Company
P. O. Box 210
Cumberland, Maryland 21501

Dr. J. H. Thacher
Allegany Ballistic Laboratory
Hercules Powder Company
Cumberland, Maryland 21501

Dr. Joshua E. Greenspon
J. G. Engr. Research Associates
3831 Menlo Drive
Baltimore, Maryland 21215

Mr. R. F. Landel
Jet Propulsion Laboratory
4800 Oak Grove Drive
Pasadena, California 91103

Mr. G. Lewis
Jet Propulsion Laboratory
4800 Oak Grove Drive
Pasadena, California 91103

Library
Newport News Shipbuilding &
Dry Dock Company
Newport News, Virginia 23607

Mr. E. A. Alexander(Research Dept.(991)
Rocketdyne Division
North American Aviation, Inc.
6633 Canoga Avenue
Canoga Park, California 91304

Mr. Cezar P. Nuguid
Deputy Commissioner
Philippine Atomic Energy Commission
Manila, Philippines

Mr. S. C. Britton
Solid Rocket Division
Rocketdyne
P. O. Box 548
McGregor, Texas 76657

Dr. A. J. Ignatowski
Redstone Arsenal Research Div.
Rohm & Haas Company
Huntsville, Alabama 35807

Dr. M. L. Merritt
Division 5412
Sandia Corporation
Sandia Base
Albuquerque, New Mexico 87115

Director
Ship Research Institute
Ministry of Transportation
700, SHINKAWA
Mitaka
Tokyo, JAPAN

Dr. H. N. Abramson
Southwest Research Institute
8500 Culebra Road
San Antonio, Texas 78206

Industry & Research Inst. (cont'd.)

Dr. R. C. DeHart
Southwest Research Institute
8500 Culebra Road
San Antonio, Texas 78206

Dr. Thor Smith
Stanford Research Institute
Menlo Park, California 94025

Dr. M. L. Baron
Paul Weidlinger, Consulting Engr.
777 Third Ave. - 22nd Floor
New York, New York 10017

Dr. T. C. Fan
The Rand Corporation
1700 Main Street
Santa Monica, California 90406

Dr. G. R. Makepeace
Director, Research & Engineering
Lockheed Propulsion Company
P. O. Box 111
Redlands, California 92374

This report was prepared as an account of Government sponsored work. Neither the United States, nor the Commission, nor any person acting on behalf of the Commission:

A. Makes any warranty or representation, express or implied, with respect to the accuracy, completeness, or usefulness of the information contained in this report, or that the use of any information, apparatus, method, or process disclosed in this report may not infringe privately owned rights; or

B. Assumes any liabilities with respect to the use of, or for damages resulting from the use of any information, apparatus, method, or process disclosed in this report.

As used in the above, "person acting on behalf of the Commission" includes any employee or contractor of the Commission, or employee of such contractor, to the extent that such employee or contractor of the Commission, or employee of such contractor prepares, disseminates, or provides access to, any information pursuant to his employment or contract with the Commission, or his employment with such contractor.

APR 2 2 1969

DATE DUE

GAYLORD PRINTED IN U.S.A.